Density-matrix renormalization group study of the bond-alternating $S=1/2$ Heisenberg ladder with ferro-antiferromagnetic couplings

J. Almeida,[1] M. A. Martin-Delgado,[1] and G. Sierra[2]
[1]*Departamento de Física Teórica I, Universidad Complutense, 28040 Madrid, Spain*
[2]*Instituto de Física Teórica, CSIC-UAM, 28049 Madrid, Spain*
(Received 24 April 2007; revised manuscript received 6 July 2007; published 21 November 2007)

We obtain the phase diagram in the parameter space $(J'/J,\gamma)$ and an accurate estimate of the critical line separating the different phases. We show several measurements of the magnetization, dimerization, nearest neighbor correlation, and density of energy in the different zones of the phase diagram, as well as a measurement of the string order parameter proposed as the nonvanishing phase order parameter characterizing Haldane phases. All these results will be compared in the limit $J'/J \gg 1$ with the behavior of the $\mathbf{S}=1$ bond alternated Heisenberg chain (BAHC). The analysis of our data supports the existence of a dimer phase separated by a critical line from a Haldane one, which has exactly the same nature as the Haldane phase in the $\mathbf{S}=1$ BAHC.

DOI: 10.1103/PhysRevB.76.184428 PACS number(s): 75.10.Jm, 74.20.Mn

I. INTRODUCTION

Quantum systems when placed in low dimensional lattices typically exhibit strongly correlated effects driving them toward regimes with no classical analog. Many properties of these regimes or quantum phases[1] depend in turn on the properties of their ground state and low-lying energy excitations.[2]

A problem of particular interest in the field of strongly correlated systems is the emergence of critical phases in a system where the generic behavior as coupling constants are varied is to be a gapped system, although those gapped phases may be of different nature. In this paper, we address this problem by selecting a system of quantum spins that allows us to perform a detailed study of critical and noncritical phases on equal footing, i.e., without any bias toward an *a priori* preferred phase. For reasons explained in Sec. II, the quantum spins are arranged in a two-leg ladder lattice[3] with antiferromagnetic Heisenberg couplings along the legs while rung couplings are ferromagnetic. In addition, we also introduce an explicit dimerization coupling in the Hamiltonian along the leg directions, which can be varied from zero to strong values. This coupling plays a major role in order to create the aforementioned critical phases out of a system with only gapped phases.

This particular type of two-leg ladder system has a number of open problems such as the precise location of critical phases in the phase diagram of the coupling constants and the nature of the gapped phases it exhibits. Our study is complete enough so as to be able to solve for these problems in a very precise manner.

The understanding of these purely quantum effects is usually a hard problem. Perturbative and variational methods in quasi-one-dimensional systems such as chains and ladders are not well suited to uncover the physics in the whole range of coupling constants involved in the description of the interactions in the system. On the contrary, the density matrix renormalization group (DMRG) method[4–8] allows us to identify the critical phases clearly and without any bias. This is so because the method is nonperturbative and allows a controllable management of errors.

Our studies have practical interest since there exist certain chemical compounds such as PNNNO and PIMNO[9] that exhibit a ladder structure with ferromagnetic couplings along the rungs. On the other hand, experiments on ladder materials have revealed a very complex behavior, such as an interplay between a spin-gapped normal state and superconductivity.[10] Moreover, a new field of study for these complex effects has been opened by the simulation of strongly correlated systems in optical lattices,[11] in particular, quantum spin chains and ladders.[12]

This paper is organized as follows. In Sec. II, we introduce the model Hamiltonian [Eq. (1)] describing a two-leg ladder lattice of spins $S=\frac{1}{2}$ with columnar bond-alternating antiferromagnetic couplings in the horizontal direction and ferromagnetic couplings in the vertical direction (see Fig. 1). We can identify some particular behaviors in appropriate weak and strong coupling limits but not for generic values of the couplings. In Sec. III, we point out the rich physical effects posed by open boundary conditions in these two-leg ladders with finite length, although it also implies an *a priori* analysis in order to find out which low-lying states contribute to the gap of the system in the thermodynamic limit. This can be done with the DMRG method by targeting several states and measuring their magnetization properties in the bulk and at the ends. Then, we compute numerically the gap (Fig. 2) and we establish the existence of a critical line in the quantum phase diagram of the model. A numerical fit of this

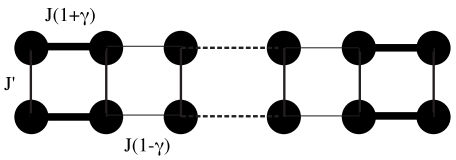

FIG. 1. Pictorial representation of the quantum Hamiltonian [Eq. (1)]. The geometry of the lattice is a two-leg ladder. Each solid dot is a spin $S=\frac{1}{2}$. In the horizontal direction (legs), we picture the bond alternation with strong links $J(1+\gamma)$ and weak links $J(1-\gamma)$. In the vertical direction (rungs), the system is arranged in the form of a columnar dimerization: strong links are parallel to one another and similarly for weak links in the lattice.

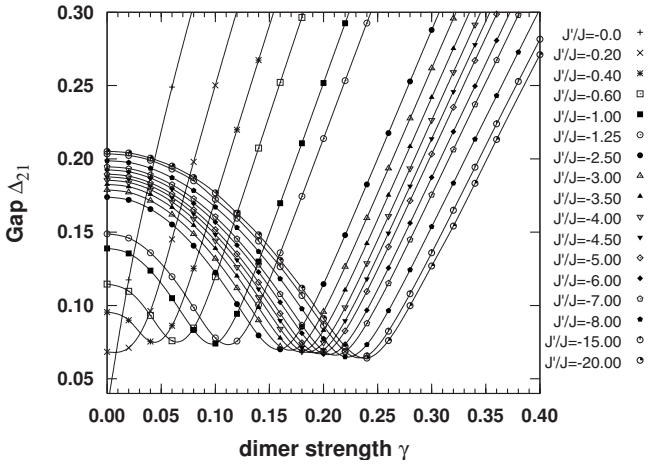

FIG. 2. Gap Δ_{21} computed on an $L=2\times 140$ ladder for different values of the parameter J'/J. Each minimum in the gap belongs to the critical line.

critical curve is also given. In Sec. IV, we determine the structure of the phase diagram by identifying the type of gapped phases occurring at each side of the critical line found in the previous section. They correspond to Haldane and dimer phases. They are identified by measuring the string order parameter and the dimerization parameter with the DMRG method. We complete our study of these phases measuring different observables. Section V is devoted to conclusions.

II. MODEL

Competing ferromagnetic versus antiferromagnetic spin interactions may give rise to critical phases if they are appropriately arranged in certain quasi-one-dimensional lattices. One emblematic example of this phenomenon is a lattice of quantum spins with the shape of a two-leg ladder such that there are antiferromagnetic couplings along the legs and ferromagnetic interactions along the rungs connecting both legs. In addition, the antiferromagnetic couplings are bond alternating in a columnar fashion. Dimerization interactions in the Hamiltonian are also known as staggered interactions. This configuration is shown in Fig. 1. More precisely, this configuration of Heisenberg-like interactions is associated with the following quantum Hamiltonian:

$$H = J \sum_{\ell=1,2} \sum_{i=1}^{L-1} [1-(-1)^i \gamma] \mathbf{S}_i(\ell) \cdot \mathbf{S}_{i+1}(\ell) + J' \sum_{i=1}^{L} \mathbf{S}_i(1) \cdot \mathbf{S}_i(2), \tag{1}$$

where $\mathbf{S}_i(\ell)$ are quantum spin $S=\frac{1}{2}$ operators located at site i of the leg ℓ and $J>0$, $J'<0$, $\gamma \in [-1,1]$ are the antiferromagnetic, ferromagnetic, and staggering couplings, respectively, as mentioned above.

Notice that several known regimes can be reached by tuning the coupling constants toward particular values. In the weak coupling limit, making $|J'/J| \ll 1$, we end up with a system consisting of two effectively decoupled $S=1/2$ bond alternated Heisenberg chain (BAHC), which are known to be gapped for every value of the dimerization parameter γ,[13] except for the point $\gamma=0$. In the strong coupling limit, making $|J'/J| \gg 1, J'<0$, the system can be effectively described by an $S=1$ spin chain with bond alternation, which is predicted to be gapped for all values of γ except for a critical point at a nonzero value γ_c.[14] These predictions are based on an approximate mapping onto the $O(3)$ σ model[15] at topological angle $\theta=2\pi S(1-\gamma)$. This yields a critical value of $\gamma_c=\frac{1}{2}$ when $\theta=\pi$ and similarly another symmetric critical value at $\gamma_c=-\frac{1}{2}$. Thus, we shall always concentrate in the region $\gamma \geqslant 0$, due to the symmetry $\gamma \leftrightarrow -\gamma$ in the Hamiltonian [Eq. (1)]. This nonlinear sigma model (NLσM) prediction misses the correct location of the critical point due to the approximations involved in that mapping. The exact location of this point has been widely studied[16] and results slightly varied depending on the approach; however, modern studies place it at $\gamma_c=0.259$,[17,18] also compatible with Fig. 5 (lower), which gives $\gamma_c=0.2590\pm 0.0001$ for a chain of 500 sites. These studies also conclude that the region $|\gamma|<\gamma_c$ corresponds to a Haldane phase, while for $|\gamma|>\gamma_c$, we move to a dimer phase. The emergence of a dimerized $S=1$ spin chain in the strong coupling limit can be explained by noting that as the rung coupling is ferromagnetic and strong $J'<0, |J'| \gg J$, the two spins $S=\frac{1}{2}$ in each rung find energetically favorable to form a spin triplet.

For generic values of the coupling constants in the Hamiltonian [Eq. (1)], this model has been the subject of a series of conjectures based on exact diagonalization numerical studies[19] in the absence of dimerization $\gamma=0$ and analytical studies using bosonization and NLσM mapping[20] in the presence of dimerization $\gamma \neq 0$. Those numerical methods only allowed to reach ladder lengths typical of $L=6$ or so, which prevents from reaching any definitive conclusion on the bulk properties of the system in the thermodynamic limit. As for the analytical studies, they conjectured the existence of a possible critical region, but due to the nature of the methods, it is not possible to give its location in terms of the original coupling constants in the model Hamiltonian [Eq. (1)].

III. CRITICAL REGION

According to the previous section, we have shown that there are strong indications for the existence of a critical curve in two limiting regimes, namely, strong and weak couplings of model (1). In this regard, one of the main issues in this model is whether it exhibits a critical line in the quantum phase diagram of J'/J vs γ or not. In this section, we address this problem using the finite DMRG algorithm and find that a critical line indeed exists in the region $0<\gamma<1$ quantitatively different from that predicted by the NLσM.

The performance of the finite DMRG algorithm is characterized by the following parameters: the number of states m retained in the truncation process of the RG method, the weight of the discarded states w_m which is a measure of the DMRG error, the number of sweeps n_s or iterations of the method after the initial warm-up process, and the tolerance ϵ of the target state energy which controls the average number of iterations that will need the diagonalization algorithm (Lanczos in our case) to compute the target state. We shall

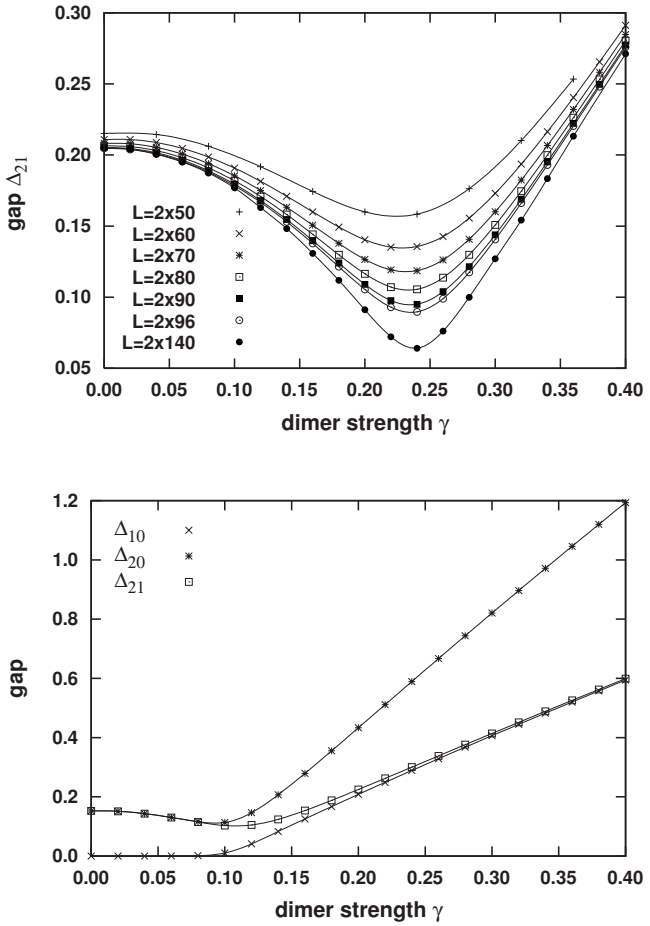

FIG. 3. Up: computation performed with an arbitrary value $|J'/J|=20$. The effect of considering finite sizes makes the minimum of the gap not to be strictly zero; however, as we take larger sizes of the system, the tendency is to lower it to zero as expected. Down: computations on an $L=2\times 96$ ladder with an arbitrary value $|J'/J|=1.250$. In the phase below the critical point, $\Delta_{21}\simeq\Delta_{20}$, while the phase above the critical point holds $\Delta_{21}\simeq\Delta_{10}$. Thereby, the gap Δ_{21} interpolates then correctly both behaviors.

provide values of these parameters in our numerical computations below.

Before applying the finite-size DMRG method, two important remarks are in order.

(i) As we shall always work with a fixed value of L, the length of the lattice, the gap $\Delta(J'/J,\gamma)$ is always finite and only in the thermodynamic limit $L\to\infty$ it may vanish for certain values of J'/J and γ, which define the critical line we are searching for. Thus, the signature of a gap in $\Delta(J'/J,\gamma)$ for fixed J'/J and varying γ will show up as a minimum in the dimerization strength parameter γ. Upon increasing the value of L, we shall obtain more robust estimations of the critical value $\gamma_c(J'/J)$ from the minima $\gamma_{\min}(L)$. In Fig. 3 (Up), we show several curves of the gap corresponding to different sizes of the system. We can observe, as explained before, that the gap is nonvanishing at the minimum but it gets lower as we let L increase and it will eventually vanish in the thermodynamic limit.

(ii) The physics of this two-leg ladder [Eq. (1)] is richer when the lattice has open boundary conditions. Moreover, the numerical performance of the DMRG method is also better under these conditions. However, open boundary conditions introduce additional degeneracies of the ground state compared to periodic boundary conditions, which force us to be careful in order to identify the gap $\Delta(J'/J,\gamma)$ we are after.

In particular, using open boundary conditions we have found that the ground state always has z-spin projection $S^z_{\rm tot}=0$, and the first excited state lies within the sector with total z-spin angular momentum $S^z_{\rm tot}=1$. Moreover, in the Haldane phase, both states converge to the same state as we increase the size of the system and so the ground state below the critical point is nearly degenerate while it is not above it, in the dimer phase. Henceforth, a finite gap in the Haldane phase only appears in the thermodynamic limit if we consider the next excited state above the first one, which has total z-spin projection $S^z_{\rm tot}=2$. The question now is whether to compute the gap as the difference of energy from the second excited state to the ground state or to the first excited state. For our purposes and considering the reasons explained next, we will use the gap $\Delta_{21}:=E_0(S^z_{\rm tot}=2)-E_0(S^z_{\rm tot}=1)$.

The reason for considering the gap Δ_{21} can be justified as follows: in the complete dimerized limit $\gamma=1$, it is clear that the difference in energy between two arbitrary consecutive levels is the same and corresponds exactly to the energy needed to promote one singlet bond to a triplet. Therefore, in this regime, Δ_{21} shall be equivalent to Δ_{10}, which is, in fact, the proper gap of the spectrum since as we said before, in the dimer region, the ground state is not degenerated. The argument for the other limit $\gamma=0$ makes use of the properties of Haldane phases, where it is known to appear as a nonbulk excitation[21] due to the existence of virtual spins at the end of the chain. Our measures suggest that the first excited state with $S^z_{\rm tot}=1$, in fact, consists on a nonbulk excitation localized in the ends contributing $S^z_{\rm nb}=1$ and the bulk itself with the same nature than the ground state contributing $S^z_b=0$ to the total magnetization. As regards the second excited state with $S^z_{\rm tot}=2$, it also has the same nonbulk excitation contributing again $S^z_{\rm nb}=1$, but now the bulk is also excited and contributes to the total magnetization $S^z_b=1$. According to this picture, the gap Δ_{10} corresponding to periodic boundary conditions has the same nature than the gap Δ_{21} with open boundary conditions since we are subtracting in the latter case the energy corresponding to the nonbulk excitations present in both states. In Fig. 3 (Down) the relation of the several possible gaps of the system is explicitly shown. From that figure, we can clearly observe the equivalence $\Delta_{21}\simeq\Delta_{20}$ in the Haldane phase and $\Delta_{21}\simeq\Delta_{10}$ in the dimer one. Moreover, $\Delta_{20}\simeq 2\Delta_{10}$ above the critical point and it is not henceforth a good quantity to measure the crossover between both phases, while Δ_{21} actually measures the correct gap in both phases.

In Fig. 4 we show rigorous comparisons of the magnetization and density of energy in the first and second excited states well into the Haldane phase with $\gamma=0$. Computations have been done on an $L=2\times 96$ ladder at the point $(J'/J=-2.5,\gamma=0)$. On the up part of the figure, we plot the mean magnetization $\langle S^z_i\rangle$ in the states with $S^z_{\rm tot}=1$ and $S^z_{\rm tot}=2$, computed in one leg of the ladder, since due to the symmetry of the Hamiltonian, the magnetization is the same in both legs.

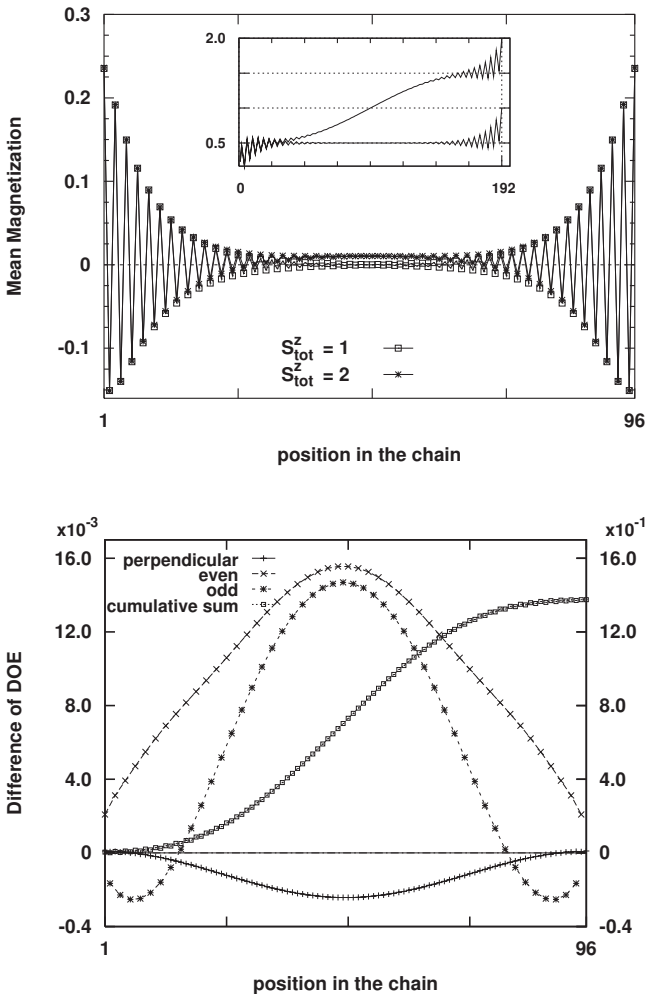

FIG. 4. Computations on an $L=2\times 96$ ladder at the point $(J'/J=-2.5, \gamma=0)$. Up: mean magnetization $\langle S_i^z\rangle$ in the states with $S^z_{\text{tot}}=1$ and $S^z_{\text{tot}}=2$, as explained in the text. Inset: cumulative sum of the magnetization over the whole extent of the ladder and the states with $S^z_{\text{tot}}=1$ and $S^z_{\text{tot}}=2$. The order of the sites in the x axis corresponds in this case to the path used to traverse the ladder in a DMRG sweep. Down: difference of energy density (DOE) of the excited states with $S^z_{\text{tot}}=1$ and $S^z_{\text{tot}}=2$: $\langle \mathbf{S}_{\ell,i}\mathbf{S}_{\ell',i'}\rangle_{S^z=2} - \langle \mathbf{S}_{\ell,i}\mathbf{S}_{\ell',i'}\rangle_{S^z=1}$. The scale on the right axis corresponds to the cumulative sum (see text for more explanations).

As a check of the accuracy of our computations, we observed that the results in both legs are the same up to the fifth or sixth decimal digit. In the inset of that figure, we show the cumulative sum of the magnetization over the whole length of the ladder and the states with $S^z_{\text{tot}}=1$ and $S^z_{\text{tot}}=2$. The order of the sites in the x axis corresponds in this case to the path used to traverse the ladder in a DMRG sweep. In the down part of this figure, we plot the difference of energy density of the excited states with $S^z_{\text{tot}}=1$ and $S^z_{\text{tot}}=2$: $\langle \mathbf{S}_{\ell,i}\mathbf{S}_{\ell',i'}\rangle_{S^z=2} - \langle \mathbf{S}_{\ell,i}\mathbf{S}_{\ell',i'}\rangle_{S^z=1}$. The difference has been divided into three contributions: the contribution labelled with *even* stands for links involving sites in the same leg and the even sublattice $(\ell'=\ell, i=2k, i'=2k+1)$, *odd* involves links joining sites in the same leg and the odd sublattice $(\ell'=\ell, i=2k-1, i'=2k)$, and *perpendicular* denotes links among legs $(\ell=1, \ell'=2, i=k, i'=k)$. The cumulative sum of the difference of the various contributions, measured in the right axis scale, is also shown. Interestingly enough, we can observe the magnetization pattern at the ends being almost identical in the states with $S^z_{\text{tot}}=1$ and $S^z_{\text{tot}}=2$. The contribution to the z-axis projection of the spin coming from the ends is equal to 1 in both cases. Notice also that the difference of the density of energy between these states is close to zero at the ends, while it becomes clearly noticeable in the bulk. All these facts strongly support the picture exposed above of a nonbulk triplet excitation with the same nature in both states, which leaves the bulk of the chain with a neat value of the projection equal to $S^z_b=0$ or $S^z_b=1$ and gives a strong hint on the equivalence of Δ_{10} with periodic boundary conditions and Δ_{21} for open systems.

After this previous analysis to identify the states needed to target the gap of the system, we present in Fig. 2 some values of the gap Δ_{21} for a ladder consisting of $L=2\times 140$ sites, at different regions of the parameter space. Computations have been performed retaining $m=300$ states of the density matrix and the grid used to explore the phase diagram is $\gamma\in[0,0.4]$, and $-J'/J=\{0.00, 0.20, 0.40, 0.60, 1.25, 2.50, 3.00, 3.50, 4.00, 4.50, 5.00, 6.00, 7.00, 10.00, 15.00, 20.00\}$. The existence of a set of minima in the function $\Delta_{21}(\gamma, J'/J)$ is clear in this graph, although they shall become more distinguishable as we move to higher values of $|J'/J|$.

As an instance of the accuracy of our results, we point out that a systematic examination of the error in each of the truncations of our DMRG computations reveals that the highest values in the whole process are of the order of $w_m \sim 10^{-8}$, and mostly they are of order $w_m \sim 10^{-10}$. To obtain a suitable accuracy in the results, we have set the number of sweeps $n_s=2$ and the tolerance to 10^{-9}. To compute the critical value $\gamma_c(J'/J)$ that minimizes the gap with enough precision, it becomes necessary to use large amount of data. In this regard, we have used interpolated values resulting from the DMRG computations.

Now, we can detect the presence of a critical line in the quantum phase diagram separating gapped phases. In Fig. 5, we plot the critical region consisting of the coordinates for each minimum in Fig. 2. In earlier studies,[16] we placed the critical point of the $S=1$ BAHC at $\gamma_c=0.259$. The curve shown in Fig. 5 shows a vertical asymptote that is still a bit off from this limiting value corresponding to the region $|J'/J|\gg 1$, but this is simply because we have chosen a value of $J'/J=-20$, which is still not big enough and also due to finite-size effects on the two-leg ladder. In the lower plots of Fig. 5, we address these possibilities by comparing our ladder in the strong ferromagnetic limit with a pure $S=1$ BAHC with different sizes. Two parameters are important in this discussion, namely, the value $\gamma_c(J'/J)$ that minimizes the gap and the value of the gap itself at this point $\Delta_{21}(\gamma_c)$. As we can observe in Fig. 2, the value of $\Delta_{21}(\gamma_c)$ does not strongly depend on the particular choice of the coupling constant ratio J'/J while it is definitely influenced by the size of the system. In Fig. 5 (lower), it is shown that the shift of γ_c computed for two $S=1$ BAHCs with different sizes, but both still large enough, is less noticeable than the difference in

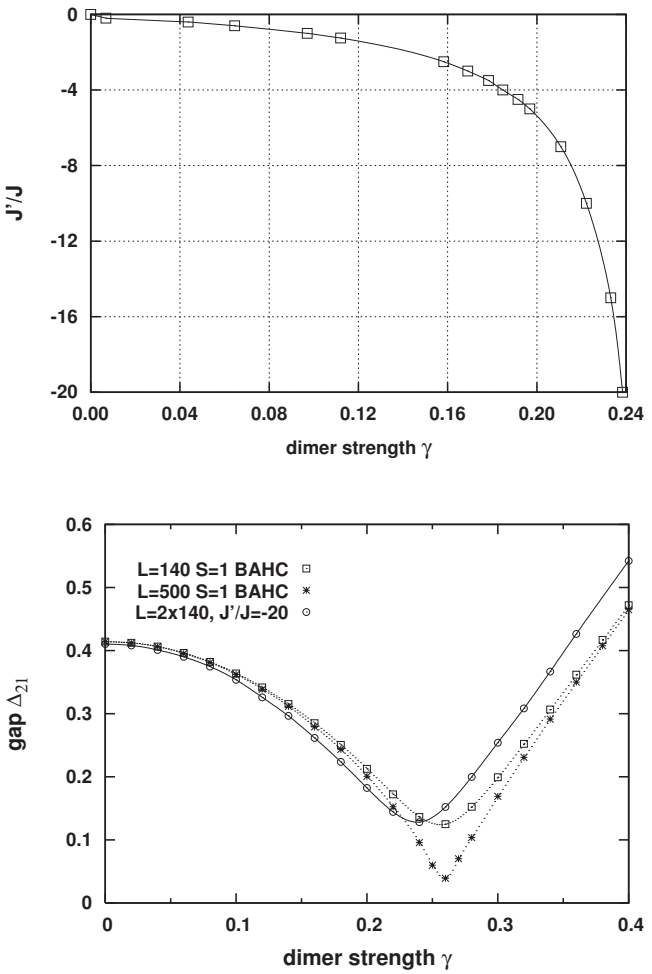

FIG. 5. Top: critical region of a ladder of size $L=2\times140$. The points of the critical line correspond to the coordinates that minimize $\Delta_{21}(\gamma,J'/J)$. The solid line is only a guide for the eyes. Bottom: the value of the minimum gap for the ladder with $L=2\times140$ sites is very similar to the corresponding $S=1$ BAHC with $L=140$ but the value of γ_c that minimizes this gap is still a bit shifted, which constitutes a signal that $J'/J=-20$ is still a low value to accurately mimic the limit BAHC behavior. The computations for the $L=500$ BAHCs were performed storing $m=450$ eigenvectors of the density matrix.

their value of $\Delta_{21}(\gamma_c)$. The similarity of this magnitude in the case of the ladder and the corresponding BAHC is clear, as well as the shift in the value of γ_c. All these make us conclude that in order to attain a better convergence with the $S=1$ BAHC and a better estimate of the critical asymptote $\gamma_c=0.259$, we shall increase the strength of the ferromagnetic coupling rather than the size of the system.

Since we have large enough data from the analysis of the critical line, we can also make a numerical estimation of the criticality curve. In Fig. 6, we present a fit of the critical curve in the region close to $\gamma_c\simeq0.259$. We choose as trial function for this fitting an inverse power law with some coefficients and exponents that are fixed by our numerics, namely,

$$J'/J=\frac{C}{(0.259-\gamma)^k}. \tag{2}$$

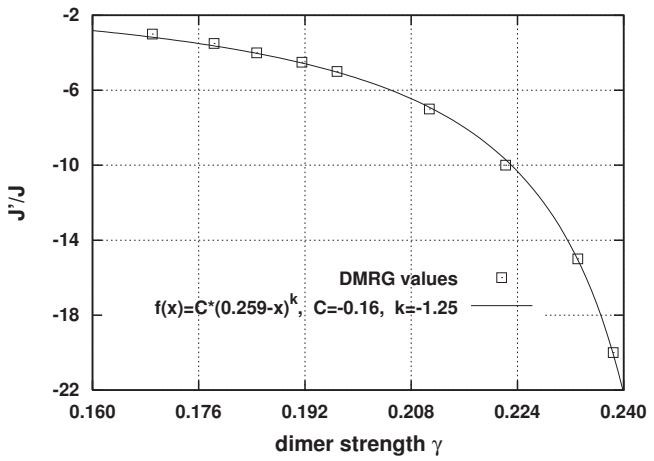

FIG. 6. The region of the critical line in the limit $|J'/J|\gg1$ fits very well to a potential function of the form $J'/J=C(0.259-\gamma_c)^k$, with $C=-0.16\pm0.01$ and $k=-1.25\pm0.01$.

The fit yields the following estimations for the values of the parameters C and k that best fit the data: $C=-0.16\pm0.01$ and $k=1.25\pm0.01$; for simplicity, the fixed value of $\gamma_c=0.259$ is taken.

IV. HALDANE AND DIMER PHASES

Once we have established the existence of a critical line in the quantum phase diagram of model (1), it is natural to wonder about the two gapped phases that this line separates, more specifically, whether they are different or not and their identification as quantum phases in the framework of strongly correlated systems.

The possible nature of those phases can be guessed from the strong ferromagnetic limit $|J'/J|\gg1$ of the ladder, effec-

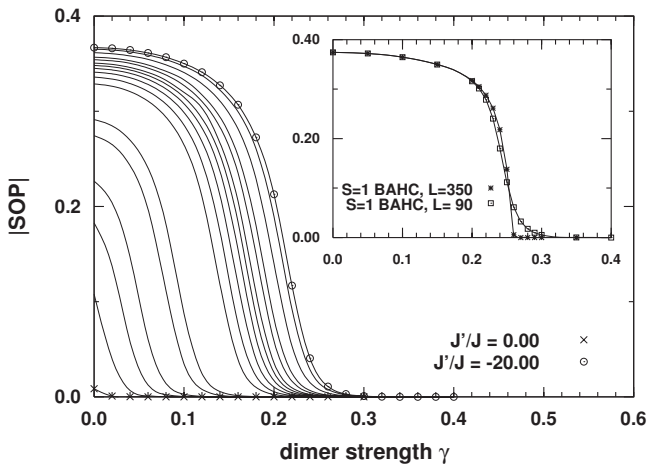

FIG. 7. String order parameter computed for a ladder consisting of $L=2\times96$ sites and $|J'/J|=\{0,0.2,0.4,0.6,1,1.25,2.5,3,3.5,4,4.5,5,6,7,10,15,20\}$. The SOP has been computed forming the triplets with adjacent $S=1/2$ spins located in different legs. The value of this parameter is nonvanishing in the Haldane phase and null in the dimer one. Inset: SOP computed for an $S=1$ BAHC. As $|J'/J|$ increases, we can observe how the ladder converges to the BAHC.

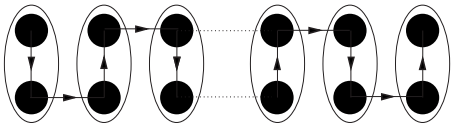

FIG. 8. A picture of the path used to compute the string order parameter in the two-leg ladder with columnar bond alternation. The ellipses mean that the sites within them are forming a triplet.

tively leading to the $S=1$ BAHC. The phases of this chain are known to be the massive Haldane phase, separated by a critical point from the massive dimer phase. To test the nature of each phase, we will make use of the order parameter in expression (3). Indeed, the Haldane phase is known to exhibit a particular hidden order that can be detected by a nonvanishing value of the order parameter, while the dimer one corresponds to a different configuration in which the order parameter is null.[22,23] The definition of this operator, denoted originally as the string order parameter (SOP), for a spin-1 chain is as follows:

$$O_{\mathrm{str}} = \lim_{|i-j|\to\infty} \left\langle S_i^z \prod_{k=i+1}^{j-1} e^{i\pi S_k^z} S_j^z \right\rangle. \tag{3}$$

This operator acting on our ground state measures how far it is from a spin liquid Néel state consisting of a sequence of $S=1$ spins such that every spin with projection $S_i^z=\pm 1$ is followed by $S_{i+k}^z=\mp 1$ and $S_{i+k'}^z=0$ for every $0<k'<k$. When we deal with $S=1/2$ particles, to compute the SOP, we have to define the pairs of particles which are most likely to couple to give a triplet and compute the SOP along the path connecting them. In our case, the existence of a ferromagnetic coupling clearly suggests that the triplets will result via this coupling. It is also worth recalling that the SOP is a parameter suited to work with translational invariant systems. In order to correctly estimate the SOP in open systems,

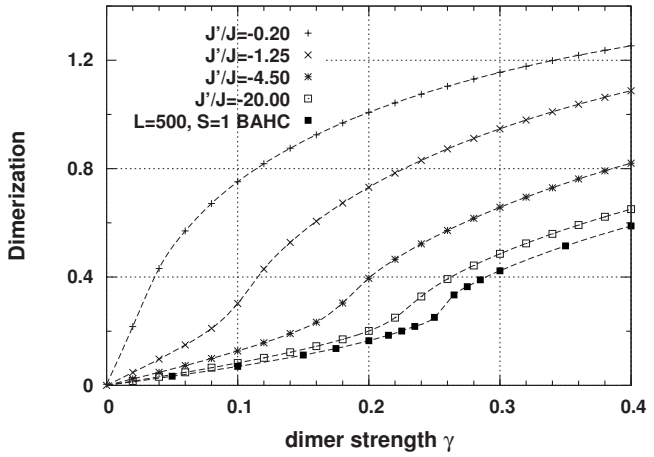

FIG. 9. Different values of the dimerization parameter $D_i := \Sigma_{\ell=1,2}\langle \mathbf{S}_{\ell,i-1}\mathbf{S}_{\ell,i}\rangle - \langle \mathbf{S}_{\ell,i}\mathbf{S}_{\ell,i+1}\rangle$ computed in the middle of a ladder of $L=2\times 96$ sites. Since we are explicitly introducing some staggering in the Hamiltonian [Eq. (1)], the dimerization parameter is nonvanishing even in the Haldane phase. However, the shape of the graphs seem to have an inflexion at the critical point. The graph corresponding to the $S=1$ BAHC has been scaled down by a factor $1/2$ due to the effective coupling constant of the ladder, which is known to be half the constant corresponding to the BAHC.

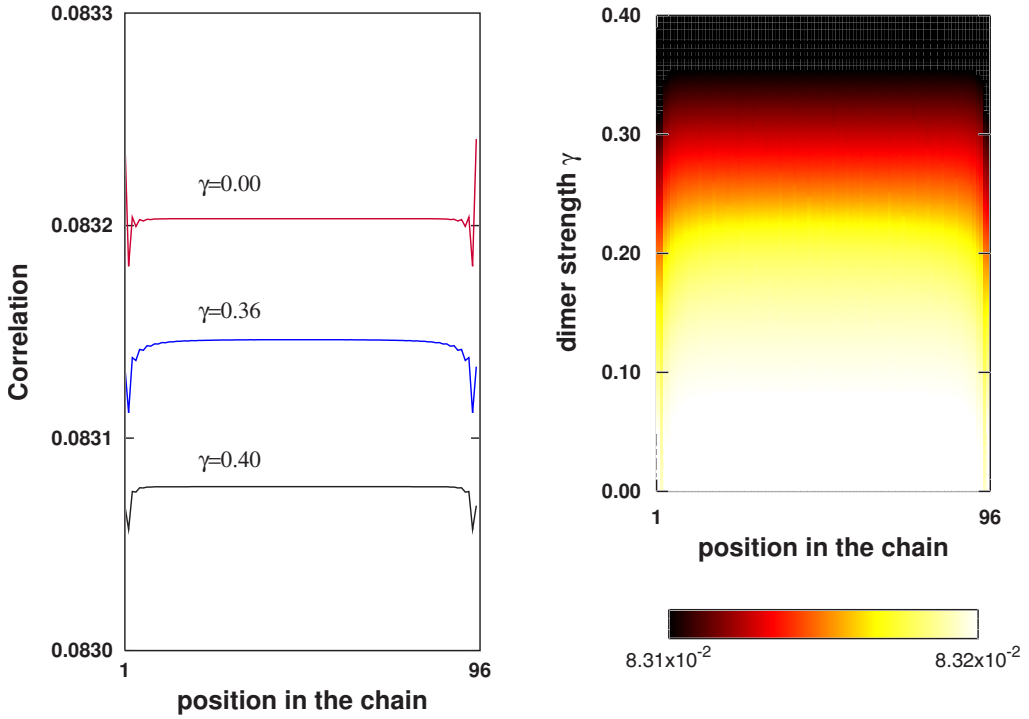

FIG. 10. (Color online) Correlation $\langle S_i^z(1)S_i^z(2)\rangle$ in the ground state of an $L=2\times 96$ site ladder and $J'/J=-20$. The plot on the left shows the correlation value for some arbitrary values of γ. The plot on the right shows the value of this magnitude in the whole region of the parameter γ.

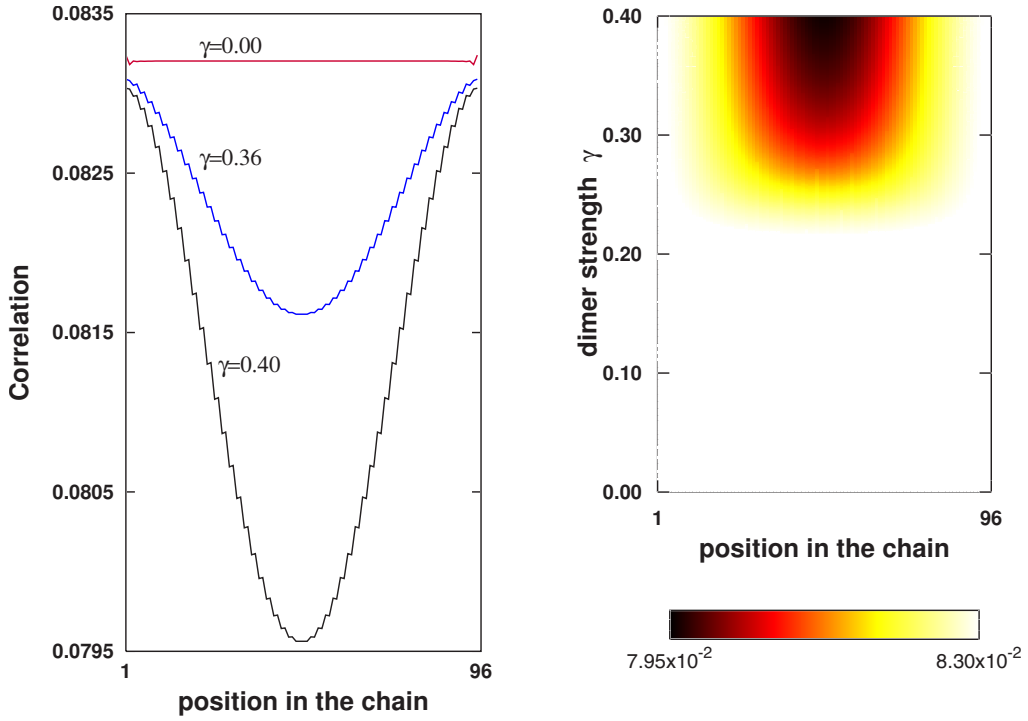

FIG. 11. (Color online) Correlation $\langle S_i^z(1)S_i^z(2)\rangle$ in the first lying excited state in the sector with $S_{\text{tot}}^z=1$ of an $L=2\times 96$ ladder and $J'/J=-20$.

we must restrict the computation to a region shorter than the whole length of the chain where end effects are negligible and only bulk physics is relevant. In Fig. 7, we show the SOP computed traversing the path shown in Fig. 8. We can observe a nonvanishing SOP below the critical point while it decays to zero above it. The inset shows the SOP computed for a $S=1$ BAHC. The resemblance between both systems as we make the ferromagnetic coupling J' stronger is apparent, as expected. For comparison, to check that the sizes used in our computations are large enough to accurately describe the

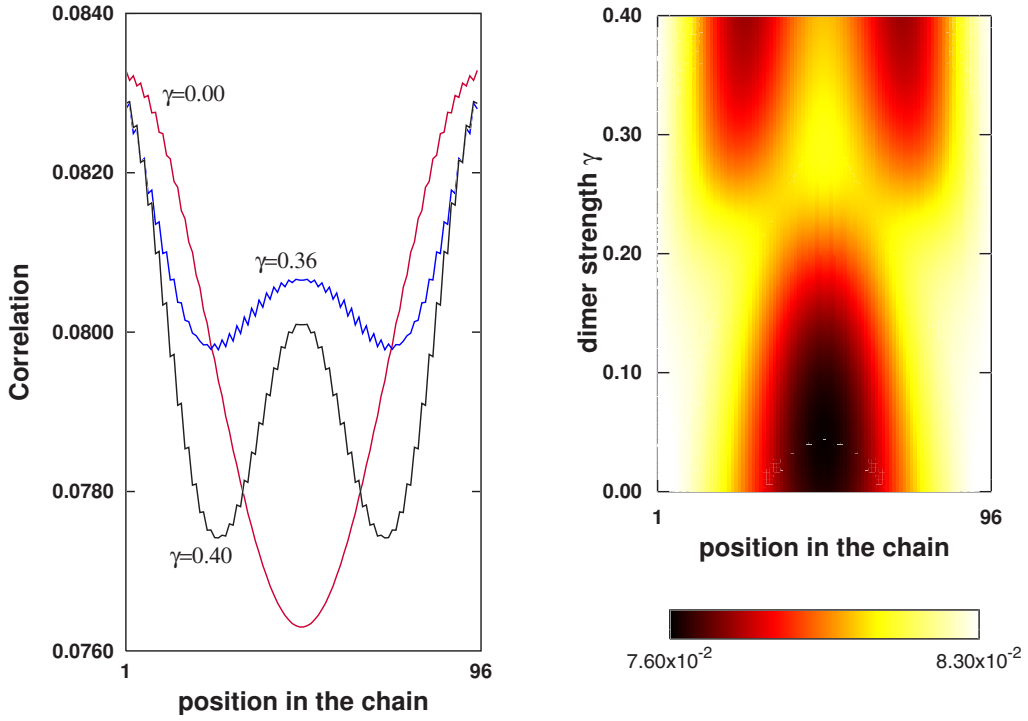

FIG. 12. (Color online) Correlation $\langle S_i^z(1)S_i^z(2)\rangle$ in the first lying excited state in the sector with $S_{\text{tot}}^z=2$ of a ladder consisting of $L=2\times 96$ sites and $J'/J=-20$.

thermodynamic limit, we draw our attention to the values of the SOP computed for $(J'/J=-20,\ \gamma=0)$ equal to 0.367 and $(J'/J=-20,\ \gamma=0.4)$ of the order of 10^{-6}. The corresponding values of an $S=1$ BAHC in the thermodynamic limit are 0.374 and zero. The fact that the string order parameter can be computed up to very high precision using relatively small systems has been widely checked in different systems, see for example Ref. 24.

From the considerations above and noting that the phases of the strong coupling limit $(|J'/J| \gg 1)$ are continuously connected with the rest of the parameter space, we can conclude therefore that the phase below the critical line in the numerical phase diagram of Fig. 2 is a gapped Haldane phase, while it is a gapped dimer phase in the region from γ belonging to the critical line to $\gamma=1$.

On the other hand, the structure of a dimer phase is such that the full translational invariance symmetry of the system is broken by one unit cell of the lattice. We want to investigate the variation of the dimerization inside the ladder as we explicitly increase the dimerization parameter γ. On this purpose, we will use the parameter

$$D_i := \sum_{\ell=1,2} \langle \mathbf{S}_{i-1}(\ell) \cdot \mathbf{S}_i(\ell) \rangle - \langle \mathbf{S}_i(\ell) \cdot \mathbf{S}_{i+1}(\ell) \rangle. \qquad (4)$$

The subindex i is necessary since open systems are intrinsically not translationally invariant. In Fig. 9 the dimerization parameter measured in the middle of the ladder is plotted. In this model, since the staggering is explicitly introduced in the Hamiltonian, the parameter defined above only vanishes at $\gamma=0$ and cannot be considered an order parameter to distinguish apart both phases as happens in other models like Majumdar-Ghosh. Nonetheless, our plots clearly exhibit different behaviors related to the convexity of the parameter at each phase. This observation indicates that an accurate estimation of the point of inflexion in the dimerization parameter could be used as a measure of the critical point between both phases.

We have also performed some measurements in the ladder to give more hints to understand the nature of both phases. Figures 10–12 show the correlation $\langle \mathbf{S}_i(1)\mathbf{S}_i(2) \rangle$ between sites in the perpendicular rungs. The pattern of the correlation can be understood by noticing that the correlation between two isolated $S=1/2$ spins coupled to give a singlet is $\langle \mathbf{S}_1\mathbf{S}_2 \rangle/3=-1/4$, while it equals $1/12$ if the spins form a triplet. From these values, we observe that the perpendicular rungs in the ground state form triplets and the distribution is uniform all along the ladder. In the excited states, however, the triplet strength of some rungs is weakened, signaling the presence of magnonlike excitations, also apparent in Fig. 13. The nature of the nonbulk excitation present in the Haldane phase is not magnonlike and that explains the different number of kinks in the Haldane and dimer phases in Figs. 11 and 12.

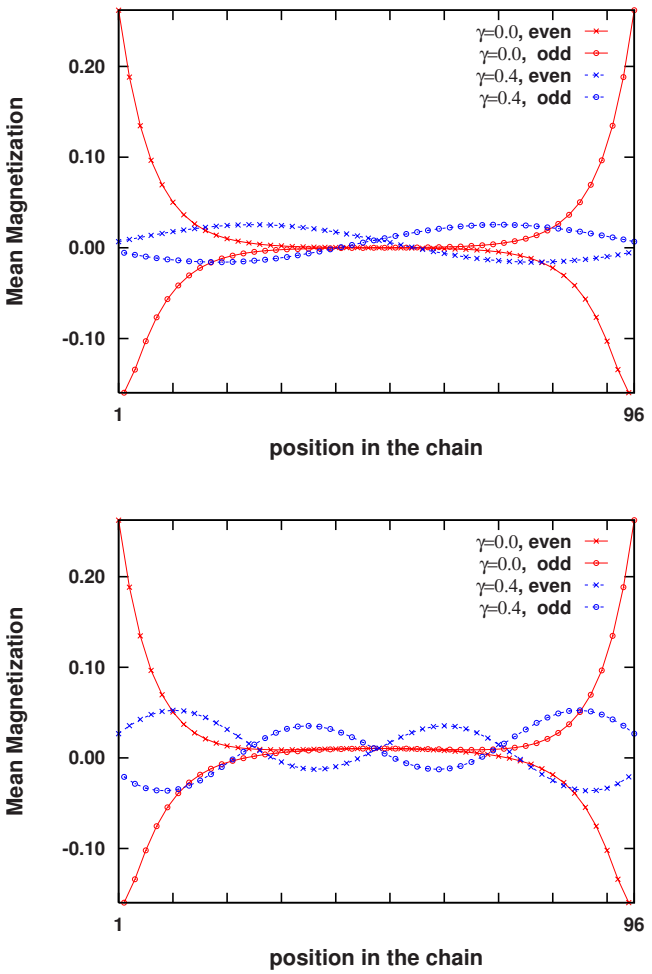

FIG. 13. (Color online) Magnetization curves in an $L=2\times96$ ladder and $J'/J=-20$ for the lowest lying states in the sectors $S^z_{\mathrm{tot}}=1$ (top) and $S^z_{\mathrm{tot}}=2$ (bottom). The curves are separated in the different sublattices consisting of the sites occupying odd or even positions. Notice that both states present a peaked magnetization at the ends for $\gamma=0.0$ well into the Haldane phase, while it vanishes in the dimer phase with $\gamma=0.4$.

V. CONCLUSIONS

We have determined the existence of a critical line in the quantum phase diagram of a two-leg ladder with columnar dimerization and ferromagnetic vs antiferromagnetic couplings. In this study, we use the finite-size system DMRG method, which allows us to give the location of that critical curve. Moreover, we have clearly identified the two phases separated by the critical line to be a Haldane phase and a dimer phase. This identification is carried out by measuring the string order parameter and the dimerization order parameter in the whole range of values of the coupling constant ratio J'/J and dimerization parameter γ.

As a by-product, we have introduced a systematic analysis of the spins at the borders of the open two-leg ladder lattice. Our model is based on $S=\frac{1}{2}$ spins, then these end-chain spins exhibit physical effects of their own. They are real spins unlike the virtual spins appearing in integer spin chains or ladders. Their physics is specially interesting when the system size is finite, and even during the process of reaching the thermodynamic limit they produce nontrivial finite-size effects along the way. These facts make the technical analysis of the opening or closing of a gap in the low-lying spectrum of a two-leg ladder with open boundary con-

ditions difficult. We have solved these difficulties by analyzing the ground state and low-lying energy excitations with respect to their bulk and boundary properties such as local magnetization and the like. With this information, it is possible to identify which states contribute to the gap in thermodynamic limit. These low-lying states have a definite total spin S^z and they can be targeted with the DMRG method. In this fashion, we have been able to identify the gapped or gapless behavior of the model within the framework of the DMRG with open boundary conditions.

ACKNOWLEDGMENTS

We thank J. Rodriguez-Laguna for useful conversations on DMRG implementations. Part of the computations of this work was performed with the High Capacity Computational Cluster for Physics of UCM (HC3PHYS UCM), funded in part by UCM and in part with FEDER funds. We acknowledge financial support from DGS grants under Contracts No. BFM 2003-05316-C02-01 and No. FIS2006-04885 and the ESF Science Programme INSTANS 2005–2010.

[1] S. Sachdev, *Quantum Phase Transitions* (Cambridge University Press, Cambridge, 1999).
[2] J. González, M. A. Martin-Delgado, G. Sierra, and A. H. Vozmediano, *Quantum Electron Liquids and High-T_c Superconductivity*, Lecture Notes in Physics, Monographs Vol. 38 (Springer-Verlag, Berlin, 1995).
[3] E. Dagotto and T. M. Rice, Science **271**, 618 (1996).
[4] S. R. White, Phys. Rev. Lett. **69**, 2863 (1992).
[5] S. R. White, Phys. Rev. B **48**, 10345 (1993).
[6] K. Hallberg, Adv. Phys. **55**, 477 (2006).
[7] A. Schollwöck, Rev. Mod. Phys. **77**, 259 (2005).
[8] *Density Matrix Renormalization*, edited by I. Peschel, X. Wang, M. Kaulke, and K. Hallberg, Lecture Notes in Physics (Springer, Berlin, 1999).
[9] Y. Hosokoshi, Y. Nakazawa, K. Inoue, K. Takizawa, H. Nakano, M. Takahashi, and T. Goto, Phys. Rev. B **60**, 12924 (1999).
[10] E. Dagotto, Rep. Prog. Phys. **62**, 1525 (1999).
[11] M. Greiner, O. Mandel, T. Esslinger, Th. W. Hänsch, and I. Bloch, Nature (London) **415**, 39 (2002); M. Greiner, O. Mandel, Th. W. Hänsch, and I. Bloch, *ibid.* **419**, 51 (2002).
[12] J. J. Garcia-Ripoll, M. A. Martin-Delgado, and J. I. Cirac, Phys. Rev. Lett. **93**, 250405 (2004).
[13] K. Hida, Phys. Rev. B **45**, 2207 (1992).
[14] I. Affleck and F. D. M. Haldane, Phys. Rev. B **36**, 5291 (1987).
[15] F. D. M. Haldane, Phys. Lett. **93A**, 464 (1982).
[16] K. Totsuka, Y. Nishiyama, N. Hatano, and M. Suzuki, J. Phys.: Condens. Matter **7**, 4895 (1995).
[17] J. Almeida, M. A. Martin-Delgado, and G. Sierra, *Lectures on the Physics of Strongly Correlated Systems XI*, AIP Conf. Proc. No. 918 (AIP, Melville, 2007).
[18] M. Kohno, M. Takahashi, and M. Hagiwara, Phys. Rev. B **57**, 1046 (1998).
[19] H. Watanabe, Phys. Rev. B **50**, 13442 (1994).
[20] K. Totsuka and M. Suzuki, J. Phys.: Condens. Matter **7**, 6079 (1995).
[21] T. Kennedy, J. Phys.: Condens. Matter **2**, 5737 (1990).
[22] M. den Nijs and K. Rommelse, Phys. Rev. B **40**, 4709 (1989).
[23] T. Kennedy and H. Tasaki, Phys. Rev. B **45**, 304 (1992).
[24] S. R. White, Phys. Rev. B **53**, 52 (1996).